Published in IET Optoelectronics
Received on 24th August 2010
Revised on 12th November 2010
doi: 10.1049/iet-opt.2010.0082

ISSN 1751-8768

Non-linear effects of intensity-modulated and directly detected optical links on receiving a linear frequency-modulated waveform

M. Shabani M. Akbari

Department of Electrical Engineering, Sharif University of Technology, Azadi Avenue, P.O. Box 11155-9363, Tehran, Iran
E-mail: makbari@sharif.edu

Abstract: Limitations imposed by the non-linearity of optical links, in the front end of a receiving array antenna, on the performance of a pulse compression radar are studied. Particularly linear frequency-modulated waveforms backscattered from a pair of targets are inspected. Inter-modulation and gain compression by noise are presented as two remarkable phenomena. For an interconnection of two dual-drive Mach–Zehnder modulators, the sensitivity of the compressed echo at the output of a matched filter receiver to certain tunable parameters is studied numerically. Finally, certain values of DC bias and phase shift between the modulators' electrodes are recommended.

1 Introduction

One of the promising methods to implement the future wideband and ultra-wideband antenna array beam-formers is through optical signal processing [1, 2]. Many different structures [3] and technologies [1, 2, 4, 5] have been proposed for optical beam-formers (OBFs), which make it essential to perform sufficient sensitivity analysis, before choosing them for a certain application. For receiving antenna array OBFs, especially for radar applications, noise and non-linearity are two critical issues. In a large array antenna, for which OBFs are more attractive choices, signal-to-noise ratio (SNR) at each antenna element is generally low. Thus, the noise and the signal may have comparable powers that necessitate a coupled analysis of noise and non-linearity. Reviewing the relevant literature, we found both issues studied rather separately, except for the recent work in [1] that has a section on performance analysis of a coherently detected single sideband (SSB) OBF structure. The mentioned report computes gain compression by noise for very small values of carrier-to-noise ratio at each antenna element. There are also reports on noise considerations, ignoring non-linearity of OBFs, for receiving arrays. In [6], the effects of a number of OBF structures are considered on the noise figure of the receiver. The effects of systematic errors in amplitude and phase of the OBF paths on a radar with a linear frequency-modulated (LFM) waveform is studied in [7], while [8] discusses the effects of noise (either correlated or uncorrelated between different channels) on the same system. A separate systematic study on the OBF non-linear effects on an LFM radar is presented in [9].

In this study we will consider receiving OBFs with intensity-modulated and directly detected (IM/DD) channels. General expressions for OBFs with dual-drive Mach–Zehnder (DDMZ) travelling wave modulators are derived considering non-linearities and system noise. The travelling wave modulators are required for wideband applications [10]. Special focus will be placed on radar receivers with LFM waveforms. We will inspect the response of a matched filter receiver to the backscattering from a pair of targets, through which we will define benchmarks for the coupled effects of non-linearity and noise in low-SNR conditions. Then we will optimise parameters of a linearised arrangement regarding those benchmarks. The proposed linearised optical link is the well-known series interconnection of two modulators.

Many OBF structures, independent of the utilised time delay mechanism, may be represented by the structure shown in Fig. 1. The performance of OBFs with wavelength division multiplexing, with a common dispersive device for the time delay implementation of all channels, may also be discussed by the presented configuration. The noise relation between the single optical links and the total OBF is discussed in detail in [6]. As the combining method is inherently a linear process, it has no effect on the non-linearity of the receiver. Thus, we will focus on a single IM/DD optical link to study the combined effects of noise and non-linearity. However, the important role of an antenna array in increasing the SNR of a single link by N (number of antenna elements) folds imposes certain conditions on this analysis. Actually we will consider low SNR values for the backscattered echo at the input of each individual optical link. As we will show, this will make the gain compression phenomena by noise remarkable.

The structure of the paper is as follows. In Section 2 we will develop a representation for the DDMZ modulator output while a pair of wideband RF signals enters it.

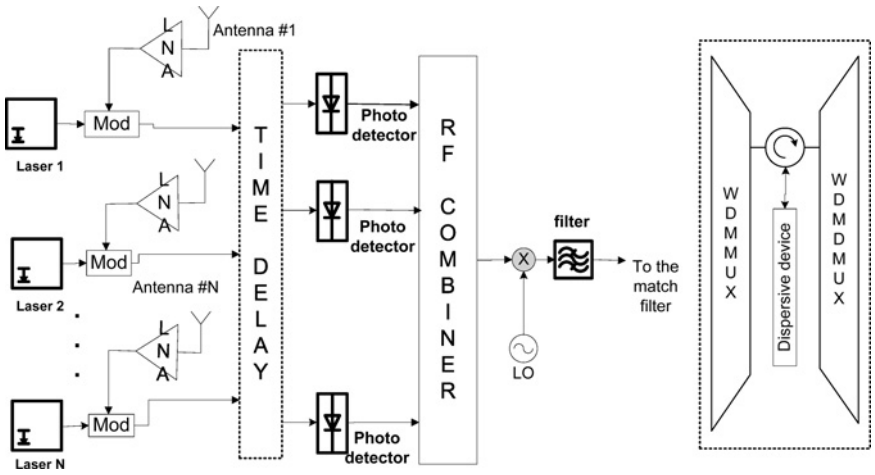

Fig. 1 *Typical structure of an OBF with IM/DD links used as a pulse compression radar receiver*
Dotted box for true time delay implementation may be replaced by the right-hand inset, as a very popular method

Section 3 provides the reader with the response of an IM/DD optical link and a matched filter receiver to a pair of returned LFM pulses. In the same section two benchmarks are introduced to characterise the quality of the receiver response. In Section 4, the serial interconnection of two modulators is examined and the parameters of the link are swept in a numerical analysis to determine optimum values with the predefined benchmarks. Section 5 concludes the paper.

2 Single-channel representation

At first, it is required to introduce basic parameters and equations for a single IM/DD channel. Let us assume that each channel has a separate optical source represented by

$$E^{i}_{\text{in}}(t) = \sqrt{2P_0}\exp\left(j\omega_0 t + j\phi(t)\right) \tag{1}$$

where P_0, ω_0 and $\phi(t)$ are the power, angular frequency and phase of the optical source. The modulated optical signal at the output of a DDMZ modulator may be represented as follows [11–13]

$$E_{mzm}(t) = \text{Re}\{\tilde{E}_{mzm}(t)\} = \text{Re}\left\{\begin{array}{l}\sqrt{2T_{ff}P_0}\exp(j\omega_0 t + j\phi(t)) \\ \times\left[\exp\left(j\gamma_1 + \dfrac{j\pi x_{\text{RF},1}(t)}{V_\pi}\right) + \exp\left(j\gamma_2 + \dfrac{j\pi x_{\text{RF},2}(t)}{V_\pi}\right)\right]\end{array}\right\} \tag{2}$$

Re represents the real part of a complex number, T_{ff} is the modulator optical loss and V_π is the DDMZ modulator switching voltage. The parameter $\gamma_m = \pi \cdot V_{\text{DC},m}/V_\pi$ is a normalised DC voltage applied to the mth ($m = 1$ or 2) electrode $x_{\text{RF},1}(t)$ and $x_{\text{RF},2}(t)$ are the RF signals applied to the first and the second electrodes, respectively. By controlling γ_1 and γ_2 and also $\Delta\varphi$, the phase shift between $x_{\text{RF},1}(t)$ and $x_{\text{RF},2}(t)$, one may generate SSB or double sideband (DSB) modulations at the DDMZ modulator output [13].

To characterise the non-linear response of the link, a pair of delayed wideband RF signals is assumed to be received. If the spectrum of the RF signal is spread around the angular frequency ω_{RF}, it may be written as follows

$$u_{\text{RF}}(t) = \sum_{k=1}^{2} A_k(t - t_k)\cos\left(\omega_{\text{RF}}(t - t_k) + \varphi_{\text{RF}}(t - t_k)\right) \tag{3}$$

To characterise noise, two terms may be added to each electrode signal; $n_{\text{in}}(t)$ representing the external noise at the input of the modulator and $n_{\text{th},m}(t)$ representing the mth travelling wave electrode ($m = 1$ or 2) thermal noise transferred to the electrode contact. Thus, assuming that the received signal (after a probable low noise amplifier (LNA)) is split equally between the two electrodes, we may write $x_{\text{RF},1}(t)$ and $x_{\text{RF},2}(t)$ as follows

$$x_{\text{RF},1}(t) = \frac{1}{\sqrt{2}}n_{\text{in}}(t) + n_{\text{th},1}(t) + \frac{1}{\sqrt{2}}\sum_{k=1}^{2} A_k(t - t_k) \times \cos(\omega_{\text{RF}}(t - t_k) + \varphi_{\text{RF}}(t - t_k)) \tag{4}$$

$$x_{\text{RF},2}(t) = \frac{1}{\sqrt{2}}\hat{n}_{\text{in}}(t) + n_{\text{th},2}(t) + \frac{1}{\sqrt{2}}\sum_{k=1}^{2} A_k(t - t_k) \times \cos(\omega_{\text{RF}}(t - t_k) + \varphi_{\text{RF}}(t - t_k) + \Delta\varphi) \tag{5}$$

In (5), $\hat{n}_{\text{in}}(t)$ is a phase-shifted version of $n_{\text{in}}(t)$ by $\Delta\varphi$. Substituting (4) and (5) into (2), we conclude the next representation for the DDMZ modulator output

$$\tilde{E}_{mzm}(t) = \sqrt{2T_{ff}P_0}\exp\left(j\omega_0 t + j\phi(t)\right) \times \left[\begin{array}{l}\exp(j\gamma_1)\exp\left(j\pi\dfrac{n_1(t)}{V_\pi}\right)\displaystyle\prod_{k=1}^{2}\left[\exp(j\beta_k\cos(\Omega_k(t)))\right] \\ +\alpha\exp(j\gamma_2)\exp\left(j\pi\dfrac{n_2(t)}{V_\pi}\right) \\ \displaystyle\prod_{k=1}^{2}\left[\exp(j\beta_k\cos(\Omega_k(t) + \Delta\phi))\right]\end{array}\right] \tag{6}$$

doi: 10.1049/iet-opt.2010.0082

where

$$\begin{aligned}\Omega_k(t) &= \omega_{\mathrm{RF}}(t-t_k)+\varphi_{\mathrm{RF}}(t-t_k)\\ \beta_k &= \pi A_k(t-t_k)/V_\pi/\sqrt{2}\\ n_1(t) &= \frac{1}{\sqrt{2}}n_{\mathrm{in}}(t)+n_{\mathrm{th},1}(t)\\ n_2(t) &= \frac{1}{\sqrt{2}}\hat{n}_{\mathrm{in}}(t)+n_{\mathrm{th},2}(t)\end{aligned} \tag{7}$$

3 Response to a pair of backscattered LFM pulses

Now we will consider the effects of a single-channel IM/DD link on the response of a matched filter receiver to a pair of backscattered LFM signals. As shown in Fig. 2, the modulated signal discussed in the previous section is passed through an ideal time delay unit and then its RF content is detected with an ideal photo-detector with responsivity R_{det}. Finally, the RF signal is down-converted to the baseband and enters a matched filter receiver. 'A network whose frequency-response function maximises the output peak-signal-to-noise power ratio is called a matched filter. This criterion, or its equivalent, is used for the design of almost all radar receivers.' [14]. Using an LFM pulse is a well-known pulse compression technique to enhance the resolution of a radar while keeping the peak power low. The matched filter output in a coherent radar receiver actually transforms time domain to range domain. Thus, the locations of the peaks of the matched filter's output represent the range of the targets.

To model an LFM signal, the amplitude and phase functions in (3) should change with time as in (8).

$$A_k(t) = V_k\,\mathrm{rect}\left(\frac{t}{T}\right),\quad \varphi_{\mathrm{RF}}(t) = \frac{\pi B}{T}t^2 \tag{8}$$

Assuming τ seconds of time delay, the photo-detector's output current may be expressed as [13]

$$i_{\mathrm{det}} = \frac{R_{\mathrm{det}}}{2}\tilde{E}_{mzm}(t-\tau)\tilde{E}^*_{mzm}(t-\tau)+i_{r\,in}(t)+i_{\mathrm{sh}}(t)+i_{\mathrm{th}}(t) \tag{9}$$

$i_{rin}(t)$, $i_{\mathrm{sh}}(t)$ and $i_{\mathrm{th}}(t)$ represent the relative intensity noise, the shot noise and the thermal noise of the detector output, respectively. Fig. 3 summarises the noise terms introduced in (7) and (9). In this analysis we assume that:

1. The received signal is weak such that a low SNR value is occurred.
2. There is an LNA after the receiving antenna which has enough gain such that the antenna and the LNA noise terms are dominant.
3. The non-linearity effects of the LNA are ignored.

The first assumption is discussed in the introduction section, the second one is rather a practical one but the

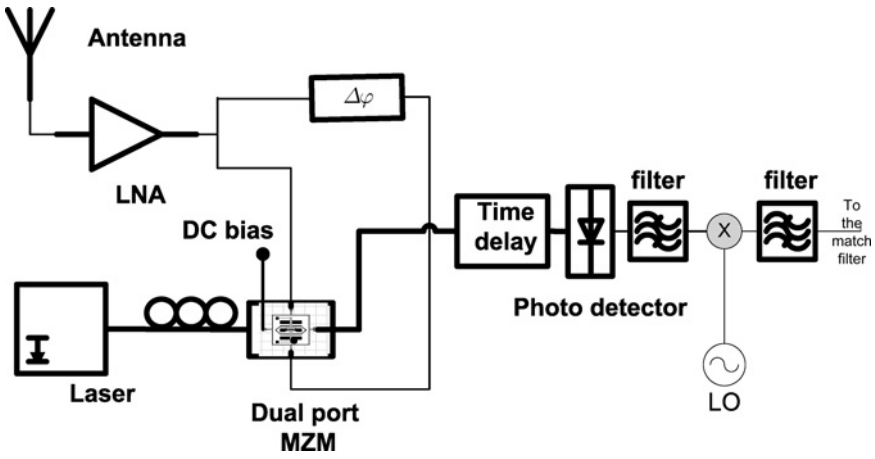

Fig. 2 *Single IM/DD optical link with a matched filter receiver*

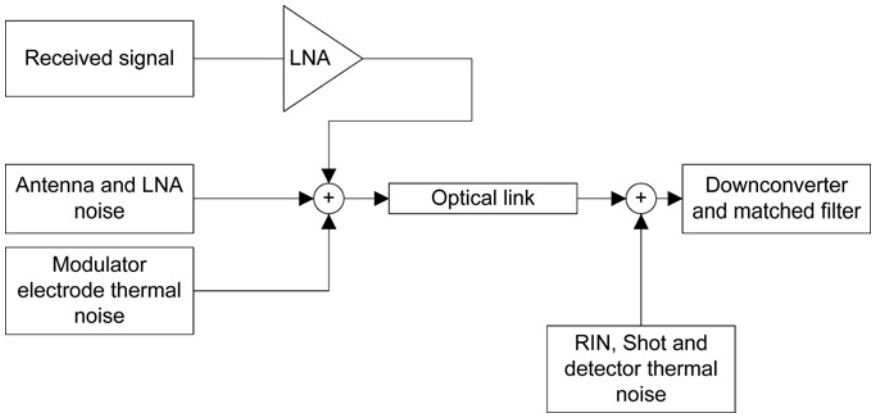

Fig. 3 *Different noises added to the signal with an optical link at the front end*

third one helps to get rid of different LNA designs, masking the optical modulator non-linearity. Optical links without pre-amplification have been recently demonstrated to be promising [15, 16]. In radar applications if the pre-amplifier is omitted the noise and signal will not be able to push the modulator into non-linear regime. Nevertheless, for a similar study on such links, we need to develop a proper non-linear noise model for travelling wave modulators that is beyond the scope of this paper.

Fig. 4 depicts the output of the matched filter to a pair of returned LFM pulses, when the SNR and the modulation index, both to be defined bellow, are about −15 and 0.24 dB, respectively. As it was noted before, we infer the ranges of the backscattering objects from the locations of peaks of the matched filter's output. The non-linearity of the receiver causes a pair of additional fake targets to appear at shorter and longer ranges.

The SNR at the input of the modulator is defined as

$$\mathrm{SNR} = \frac{P_{\mathrm{sig}}^{\mathrm{av}}}{N_{\mathrm{in}}} \tag{10}$$

in which N_{in} represents the noise power at the modulator's input and $P_{\mathrm{sig}}^{\mathrm{av}}$ is the average power of the received signal. For a pair of backscattered LFM pulses, introduced in (3) and (8), with a pulse repetition frequency of f_{prf}, we have

$$P_{\mathrm{sig}}^{\mathrm{av}} = f_{\mathrm{prf}} \int_T (u_{\mathrm{RF}}^i(t))^2 \, \mathrm{d}t \tag{11}$$

We also define the modulation index as follows to match the custom definition for sinusoidally modulated signals [9]:

$$m = \frac{\sqrt{2P_{\mathrm{sig}}^{\mathrm{av}}}\pi}{V_\pi} \tag{12}$$

In Fig. 4, two new parameters are also introduced, peak side-lobe level (PSL) and peak-to-noise ratio (PNR). The PSL value is the minimum difference between the peak points of the real targets and the fake ones appearing because of receiver non-linearities, in the compressed echo response, in decibels. The parameter PNR is just the difference between the largest magnitude and the average noise level in the received compressed echo.

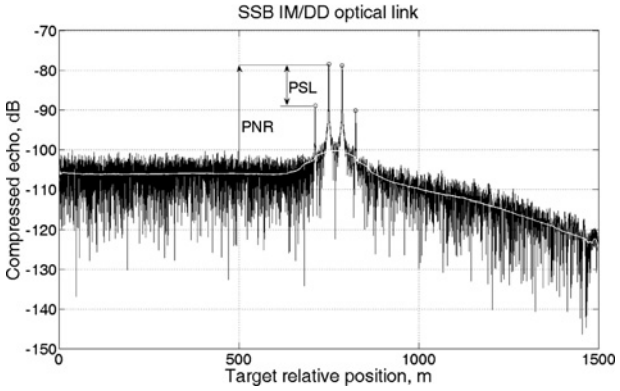

Fig. 4 *Matched filter output of a receiver with an optical link in the front end showing backscattering from two targets*

SNR is assumed to be −15 dB and the LNA and the antenna noises to dominate other noise terms. The modulation index is assumed to be about 0.24. The average noise level is computed by performing a moving average on the compressed echo

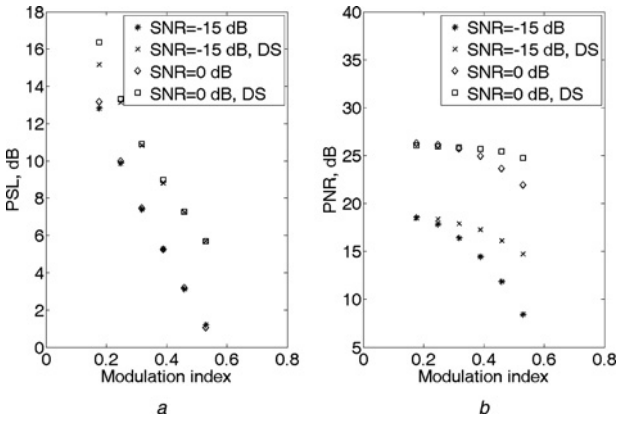

Fig. 5 *PSL and PNR of the matched filter output for two different SNR values and for two different structures*

SNR values are chosen to be 0 and −15 dB. The two structures are those of Figs. 2 and 6. DS stands for double-series interconnection of two modulators

Fig. 5 shows PSL and PNR values for the compressed echo response to a pair of LFM pulses with equal powers at the receiver input of Fig. 2. The figure is plotted for two different SNR values of −15 and 0 dB. It is worth mentioning that the plots in both Figs. 4 and 5 are results of averaging over 50 time-domain Monte Carlo simulations and the modulations are SSB.

Fig. 5*a* shows that the SNR has no remarkable effect on the PSL, while it decreases substantially with increasing modulation index. On the other hand, Fig. 5*b* shows that the PNR values decrease remarkably for the lower SNR case with increasing modulation index. This is actually a gain compression effect owing to noise. The RF signal detected at the optical link output has three main parts in a non-linear regime:

1. A copy of the signal
2. Noise and its self-modulations
3. Signal modulated by noise

In the absence of the third term and with an additive Gaussian-distributed noise, the matched filter would be the best filter to extract the signal from noise. However, in the non-linear regime the second and the third terms are not ignorable. Especially when the noise is a large signal, the RF signal will be modulated by a random process and the matched filter output quality degrades. As shown in Fig. 5*b* the further we increase the modulation index, the harder it is to distinguish targets from noise.

4 Series interconnection of two modulators

The series interconnection of two Mach–Zehnder modulators is a way to linearise an optical link, especially for application with less than an octave bandwidth [10]. Fig. 6 shows a single IM/DD optical link, similar to Fig. 2, with such a linearised configuration. Four parameters in this structure may be tuned to control the output compressed echo: the phase shifts between the two electrodes of the modulators ($\Delta\varphi_1$, $\Delta\varphi_2$) and also the DC biases of the modulators ($\Delta\gamma_1$, $\Delta\gamma_2$). The latter two parameters are related to the aforementioned γ_1 and γ_2 as follows

$$\Delta\gamma_m = |\gamma_{1\,m\text{th modulator}} - \gamma_{2\,m\text{th modulator}}|, \quad m = 1, 2 \tag{13}$$

doi: 10.1049/iet-opt.2010.0082

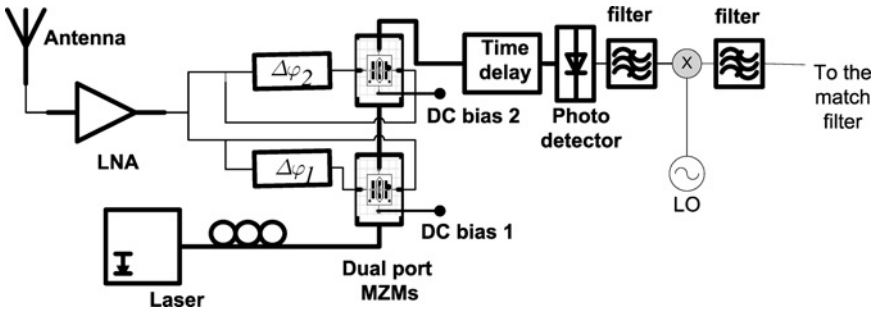

Fig. 6 *Series interconnection of two Mach–Zehnder modulators in a single IM/DD optical link*

Fig. 5 illustrates the effect of the double-series interconnection of two modulators on PNR and PSL values compared to the previously described data of the optical link with a single modulator. The provided results are plotted for $\Delta\varphi_1 = \Delta\varphi_2 = \Delta\gamma_1 = \Delta\gamma_2 = \pi/2$. The improvement in PSL is obvious, compared to the single-modulator case. The gain compression by noise, which is reflected in PNR, is also reduced by means of this linearisation technique.

4.1 Sensitivity analysis

By changing the phase shift between the two DDMZ modulator electrodes and also the DC bias of each arm, we will analyse the variations of the PSL and the PNR at the output. Contour plots showing the effect of $\Delta\varphi_1$ and $\Delta\varphi_2$ parameters in a double-series interconnection of two DDMZ modulators on PSL and PNR are plotted in Figs. 7*a* and *b*, respectively. In both plots we have chosen $\Delta\gamma_1 = \Delta\gamma_2 = \pi/2$, that is, both modulators are biased at quadrature. It is seen that both PSL and PNR values increase towards the $\Delta\varphi_1 = \Delta\varphi_2 = \pi/2$ point which both modulators produce SSB intensity modulations. However, the next contour plots in Fig. 8 reveals that biasing modulators away from quadrature (here at $\Delta\gamma_1 = \Delta\gamma_2 = 3\pi/4$) will make the PSL values increase but the PNR values to decrease. Although the rising trend towards the $\Delta\varphi_1 = \Delta\varphi_2 = \pi/2$ point is repeated. Results depicted in Fig. 8 show that the PSL and PNR dependence on phase shift behave differently. To clarify this, in Fig. 9 we have swept DC bias values of the two modulators while fixing $\Delta\varphi_1 = \Delta\varphi_2 = \pi/2$. The right plot confirms that the $\Delta\varphi_1 = \Delta\varphi_2 = \pi/2$ and the $\Delta\gamma_1 = \Delta\gamma_2 = \pi/2$ conditions give maximum PNR values, but this is not true

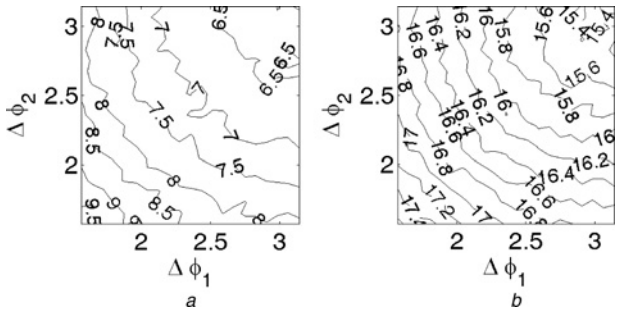

Fig. 7 *Contour plots showing the effect of $\Delta\varphi_1$ and $\Delta\varphi_2$ parameters on a double-series connection of two DDMZ modulators*

a PSL
b PNR
In both plots $\Delta\gamma^1 = \Delta\gamma^2 = \pi/2$

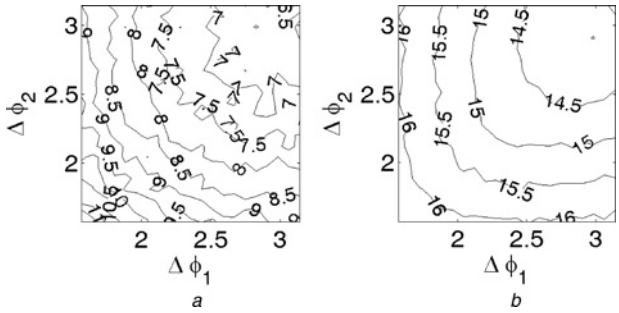

Fig. 8 *Contour plots showing the effect of $\Delta\varphi_1$ and $\Delta\varphi_2$ parameters on a double-series interconnection of two DDMZ modulators*

a PSL
b PNR
In both plots $\Delta\gamma^1 = \Delta\gamma^2 = 3\pi/4$

for PSL values. The left diagram illustrates that the optimum PSL conditions are met for some DC bias pairs around $(\Delta\gamma_1, \Delta\gamma_2) = (0, \pi)$ or $(\Delta\gamma_1, \Delta\gamma_2) = (\pi, 0)$. The different behaviour of PSL and PNR with sweeping phase shift and bias parameters is related to their different origins. PSL is a parameter that is not dependent on noise. The two modulators, when biased at different points, produce higher-order harmonics that may cancel each other. The stronger this cancellation occurs, the larger PSL is achieved. On the other hand, PNR increases when the noise and signal inter-modulations and also noise self-modulation terms shrink. This does not necessarily occur strongly at the same conditions in which PSL grows.

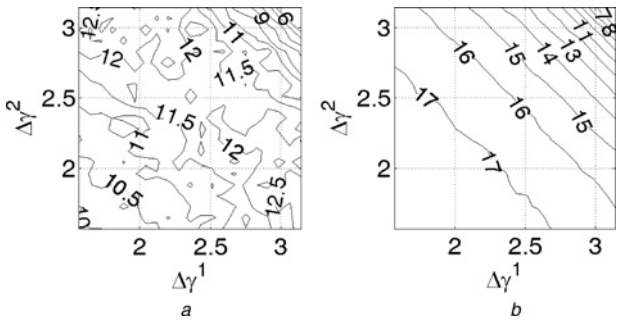

Fig. 9 *Contour plots showing the effect of $\Delta\gamma^1$ and $\Delta\gamma^2$ parameters in a double-series interconnection of two DDMZ modulators*

a PSL
b PNR
In both plots $\Delta\varphi^1 = \Delta\varphi^2 = \pi/2$

It is also seen from the contour plots that using a pair of single-drive Mach–Zehnder modulators, which is characterised by $\Delta\varphi_1 = \Delta\varphi_2 = \pi$, has the worst performance regarding both PSL and PNR. This is a satisfying reason for choosing more complex and more expensive dual-drive modulators.

All plots in Figs. 7–9 are results of the previously presented formulation in Section 2, with averaging over 50 Monte Carlo simulations. The SNR is assumed to be −15 dB with its definition given in (10). The LFM signal has got a 10% fractional bandwidth around the RF carrier and the modulation index is around 0.35.

5 Conclusions

As the dynamic range of a radar receiver is an important factor in evaluating its performance, we have studied the effects of non-linearity and noise of IM/DD optical links in its front end. Optical links may be used in either antenna remote control or beam-forming networks of large antenna arrays. In the latter case, a low-SNR condition is very possible at the array element level, before the array factor could increase it. It is shown in this paper that in low-SNR conditions the non-linearity of the front-end optical modulator has certain effects on the matched filter's output. At this output different targets are resolved in range and cross section. The non-linearity of the optical front end causes fake targets to appear. The amount of the tolerable magnitude of fake targets is reflected in the PSL parameter in the presented analysis. Moreover modulation of the backscattered signal by a large amplified noise causes a gain compression phenomenon. Actually, the interaction of a large random noise with the signal deteriorates the ability of the matched filter to extract the signal from noise. This is reflected in the PNR parameter in the presented analysis. To quantify these parameters in a pulse compression radar with a matched filter receiver, we considered pulses backscattering from two distinct targets. This is inspired from the well-known two-tone test in non-linear RF circuits.

There are different ways to linearise an optical modulation process and achieve a larger dynamic range. We chose a series interconnection of two dual-drive optical modulators. This interconnection provides four tunable parameters, that is, two DC bias values and two phase shift values between each modulator RF drives. The structure was inspected numerically to find optimum conditions regarding the aforementioned PNR and PSL benchmarks. Contour plots of both PNR and PSL are calculated and plotted to visualise their variations. PNR values seem to increase towards $\Delta\varphi_1 = \Delta\varphi_2 = \pi/2$ and $\Delta\gamma_1 = \Delta\gamma_2 = \pi/2$ but the trend for PSL values are not similar. Fixing the DC bias of the two modulators to equal each other, the PSL values increase towards $\Delta\varphi_1 = \Delta\varphi_2 = \pi/2$. However, unequal DC bias conditions of the two modulators at $(\Delta\gamma_1, \Delta\gamma_2) = (0, \pi)$ or $(\Delta\gamma_1, \Delta\gamma_2) = (\pi, 0)$ provides larger PSL values. These different trends of PSL and PNR values are the results of their different origins. PSL increases when the higher-order components produced by the two modulators cancel each other, regardless of noise. PNR, at the other hand, increases when the signal modulated by noise and noise self-modulations decrease. As a single-drive modulator may be modelled as a special case of a dual-drive one, it was shown that it provides the worst conditions regarding both PSL and PNR.

6 References

1 Meijerink, A., Roeloffzen, C.G.H., Meijerink, R., *et al.*: 'Novel ring resonator-based integrated photonic beamformer for broadband phased array receive antennas – part I: design and performance analysis', *J. Lightwave Technol.*, 2010, **28**, (1), pp. 3–18

2 Jofre, L., Stoltidou, C., Blanch, S., *et al.*: 'Optically beamformed wideband array performance', *IEEE Trans. Antennas Propag.*, 2008, **56**, (6), pp. 1594–1604

3 Ritosa, P., Batagelj, B.: 'Overview of optically driven antenna systems'. Proc. SPIE – Int. Society for Optical Engineering, Yalta, 2008

4 Yao, S.B.J.: 'Photonic true-time delay beamforming based on superstructured fiber bragg gratings with linearly increasing equivalent chirps', *J. Lightwave Technol.*, 2009, **27**, pp. 1147–1154

5 Sagues, M., Loayssa, A.: 'Optical beamforming for phased array antennas using stimulated Brillouin scattering'. Int. Topical Meeting on Microwave Photonics 2009 (MWP09), Valencia, Spain, 2009

6 Froberg, N.M., Ackerman, E.I., Cox III, C.H.: 'Analysis of signal to noise ratio in photonic beamformers'. IEEE Aerospace Conf. Proc., Big Sky, MT, 2006

7 Rotman, R., Raz, O., Barzilay, S., Rotman, S., Tur, M.: 'Wideband antenna patterns and impulse response of broadband RF phased arrays with rf and photonic beamforming', *IEEE Trans. Antennas Propag.*, 2007, **55**, (1), pp. 36–44

8 Rotman, R., Rotman, S., Tur, M.: 'Noise considerations for wideband true time delay photonic beamformers'. IEEE Radar Conf. 2008 (RADAR '08), Rome, Italy, 2008, pp. 1–6

9 Yaron, L., Rotman, R., Tur, M.: 'The impact of RF nonliniearities in an optical link on the contrast of imaging radars'. Int. Topical Meeting on Microwave Photonics 2009 (MWP '09), Valencia, Spain, 2009, pp. 1–4

10 Cox, C.H.: 'Analog optical links: theory and practice' (Cambridge University Press, New York, 2004), pp. 99–101, 244

11 Cho, T.S., Kim, K.: 'Effect of third-order intermodulation on radio-over-fiber systems by a dual-electrode Mach–Zehnder modulator with ODSB and OSSB signals', *J. Lightwave Technol.*, 2006, **24**, (5), pp. 2052–2058

12 Chen, X., Feng, S., Huang, D.: 'Impact of Mach–Zehnder modulator chirp on radio over fiber links', *J. Infrared Millim. Terahertz Waves*, 2009, **30**, (7), pp. 770–779

13 Corral, J.L., Marti, J., Fuster, J.M.: 'General expressions for IM/DD dispersive analog optical links with external modulation or optical up-conversion in a Mach-Zehnder electrooptical modulator', *IEEE Trans. Microw. Theory Tech.*, 2001, **49**, (10 Part 2), pp. 1968–1976

14 Skolnik, M.I.: 'Introduction to radar systems' (McGraw-Hill, 1980, 2nd edn.), p. 369

15 Ackerman, E.I., Burns, W.K., Betts, G.E., *et al.*: 'RF-Over-fiber links with very low noise figure', *J. Lightwave Technol.*, 2008, **26**, (15), pp. 2441–2448

16 Ackerman, E.I., Betts, G.E., Burns, W.K., Cox, C.H., Phillips, M.R., Roussell, H.: 'Low-noise-figure photonic links without pre-amplification'. IEEE Sarnoff Symp. 2009 (SARNOFF '09), Princeton, NJ, USA, 2009, pp. 1–4

doi: 10.1049/iet-opt.2010.0082